URSI GASS 2023, Sapporo, Japan, 19 – 26 August 2023

Novel 4×4 PIFA Antenna Module Covering Bands N78/N79 of 3.40-3.60 and 4.80-4.90 GHz for 5G Mobile Terminals

Le Chang* (1) and Xiaomin Chen (2)
(1) Xi'an Jiaotong University, Xi'an, China; e-mail: changle@xjtu.edu.cn
(2) Inner Mongolia University, Hohhot, China; e-mail: chenxiaomin_ee@163.com

Abstract

To meet the high communication specification of the 5G era and release the huge pressure on the terminal's bezel, a novel approach for dual-band planar antenna with low profile property is proposed. Four identical dual band PIFAs are arranged in a sequentially rotated style and each antenna element is a slotted quasi-quarter circle with two edges shorted and one edge left open. A one-eight quasi-TM_{11} mode of the circular patch and a quasi-$TM_{0,0.5}$ mode of the half-mode patch is excited to cover two Chinese 5G bands. The realized antenna operating at partial 5G Bands N78 (3.40-3.60 GHz) and N79 (4.80-4.90 GHz) is with a profile of only 1.2 mm, about 0.014 λ_L (λ_L refers to the wavelength of the lowest frequency in the -6 dB operating band). Measured results of the fabricated prototype show that the -6 dB impedance bandwidths are 3.43-3.68 GHz (250 MHz, 7.0%) and 4.76-4.93 GHz (170 MHz, 3.5%) with average total efficiencies of -1.9 dB (64.3%) and -2.9 dB (51.3%) at the lower and higher bands, respectively. The isolations are better than 11.5 dB and 21.9 dB for the lower and higher bands, respectively. All the ECCs are lower than 0.30.

1 Introduction

5G has experienced a boom time since 2019. The most distinctive differences between 5G and 1G-4G are the enhanced communication specifications, namely 4×4/8×8 MIMO, which make the antenna number in modern mobile terminals proliferate sharply. The antenna number increases sharply from about 4G's 4 to 5G's 20 and almost all the mobile antennas are implemented on metallic bezels [1]-[5]. However, smartphone design manufacturers began to place electronic components with larger sizes inside the smartphone such as large imaging systems, batteries, speakers, etc., which squeezed the space originally belonging to the antenna. This puts a lot of pressure on the smartphone bezels and restricts the performance and advancement of the mobile antenna.

Recently, scholars have been looking into new spaces for the antenna deployment of mobile terminals. The mobile terminal's back cover is an unused region that can offer a large, flat area for deploying planar-type antennas. As a result, planar back cover integrated patch antenna has been started studying recently [6], [7].

The author classifies the design ideas of dual-band patch antennas into three categories. The first type is constructing two resonant structures, such as by using stub-loading structure [8] or slotted patch [9]. In [8], two unequal stubs of the M-shaped patch resonate at different frequencies. In [9], the dual-band antenna is design by producing extra resonance operating with the slot mode. The second type is to add parasitic resonant structures [10]-[12]. In [11], shorting parasitic patches are added beside the main patch to overcome the narrow bandwidth characteristic of the patch antenna. In [12], the parasitic patch is excited through electric coupling, and the impedance bandwidth is tripled. The third resorts to higher-order modes of different patch antennas [13], [14]. In [13], by loading stub and cutting slot, a triple-band rectangular patch antenna using the fundamental TM_{10} mode together with modified TM_{20} and TM_{30} modes is realized. In [14], An omnidirectional dual-band dual circularly polarized antenna with wide beam radiation patterns using TM_{01} and TM_{02} modes is investigated. However, not all of the antennas mentioned in these references have low-profile characteristics.

In this paper, slotted planar inverted-F antenna (PIFA) is adopted as a dual-band element. The proposed dual-band four-antenna module covering partial 5G bands N78 (3.40-3.60 GHz) and N79 (4.80-4.90 GHz) is with a radius of 52 mm and a low profile of 1.2 mm. Measured results have verified the design strategy.

2 Dual-Band 4×4 Antenna Module

2.1 Proposed Antenna Structure

Fig. 1 shows the (a) exploded, (b) side, and (c) plain views of the proposed dual-band 4×4 antenna module. As shown in Fig. 1 (a) and (b), the proposed antenna consists of three parts, including the antenna substrate, air layer, and ground substrate; the total effective profile of the proposed antenna module is 1.2 mm, consisting of 0.7-mm-thick air layer and 0.5-mm-thick FR-4 layer (εr=4.4, tanδ=0.02).

As shown in Fig. 1 (c), the antenna module consists of four slotted PIFA elements that are arranged in a sequentially rotated style. Each element is approximately a quarter circle with two straight edges and one arc-shaped edge, where one of the straight edges is shorted by eight metallic pins and the curve edge is shorted by one metallic pin. In

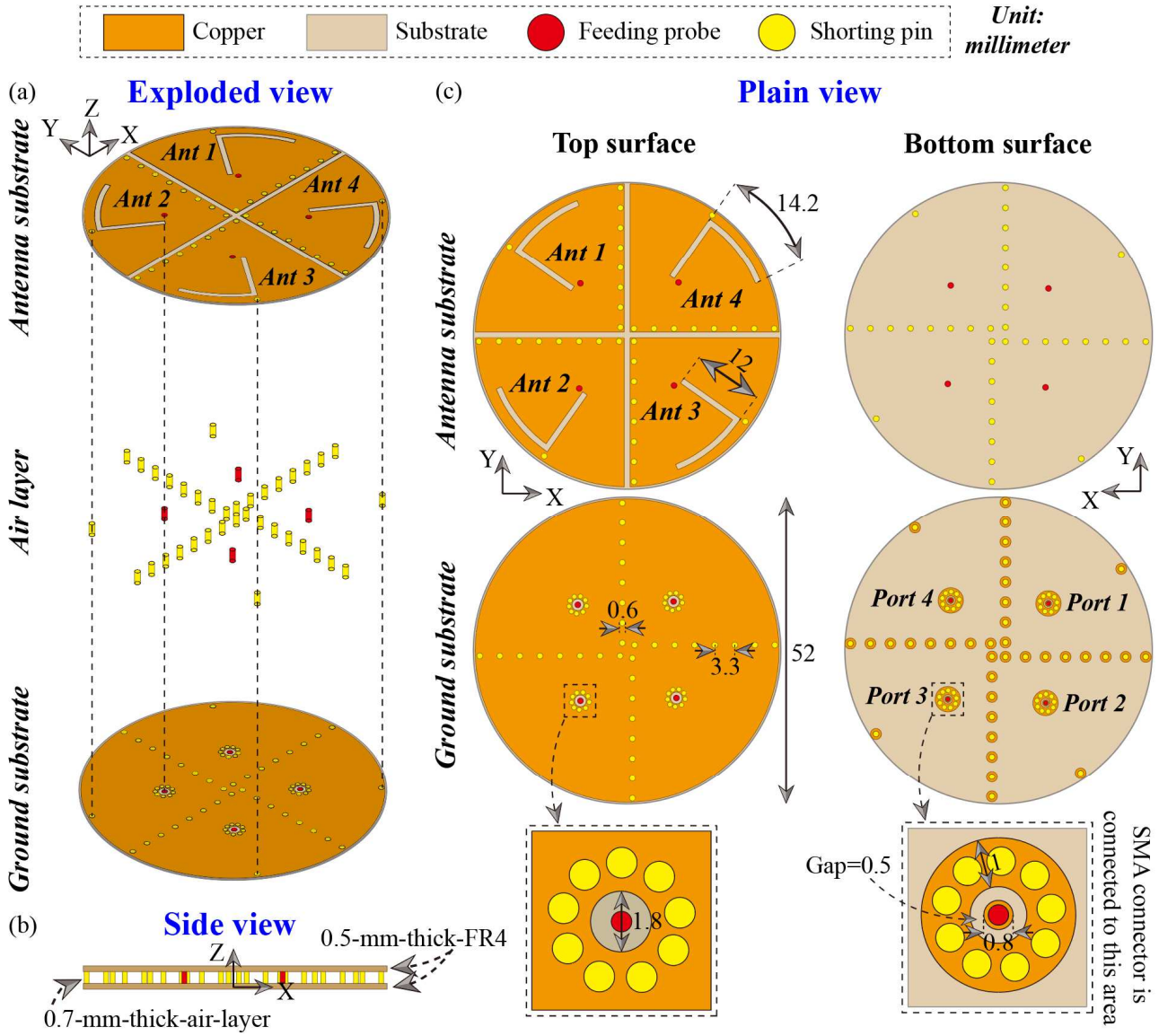

Fig. 1. (a) Exploded, (b) side, and (c) plain views of the proposed dual-band 4×4 antenna module.

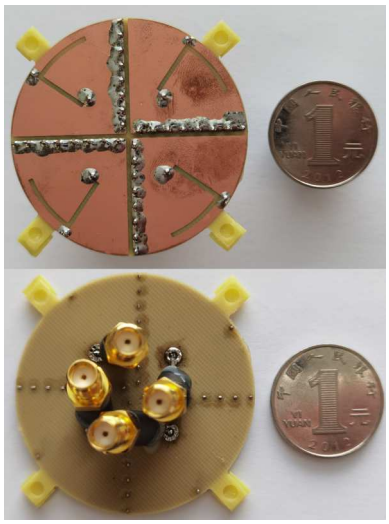

Fig. 2. Photograph of the fabricated protype (compared to a Chinese one-yuan coin).

the middle of the PIFA, there is an L-shaped slot. The inner conductor of the feeding cable is connected to the radiating aperture through the feeding probes. The dimension of the proposed antenna module is $\pi \times 26^2$ mm^2.

2.2 Results

The full-wave simulation software CST (version 2020) is used to simulate the proposed 4×4 antenna module. To verify the feasibility, a fabricated prototype is measured and its comparison with a Chinese one-yuan coin is shown in Fig. 2. The simulated and measured results are presented in Fig. 3 (a) and (b), respectively.

Due to rotation symmetry, only the parameters related to Ant 1 are given in the simulated one. Two resonance frequent points can be observed at 3.50 GHz and 4.84 GHz, as can be seen from the $|S_{11}|$ curve, and the -6 dB impedance bandwidths are 3.39-3.60 GHz (210 MHz, 6.0%) and 4.77-4.92 GHz (150 MHz, 3.1%). The average total efficiency

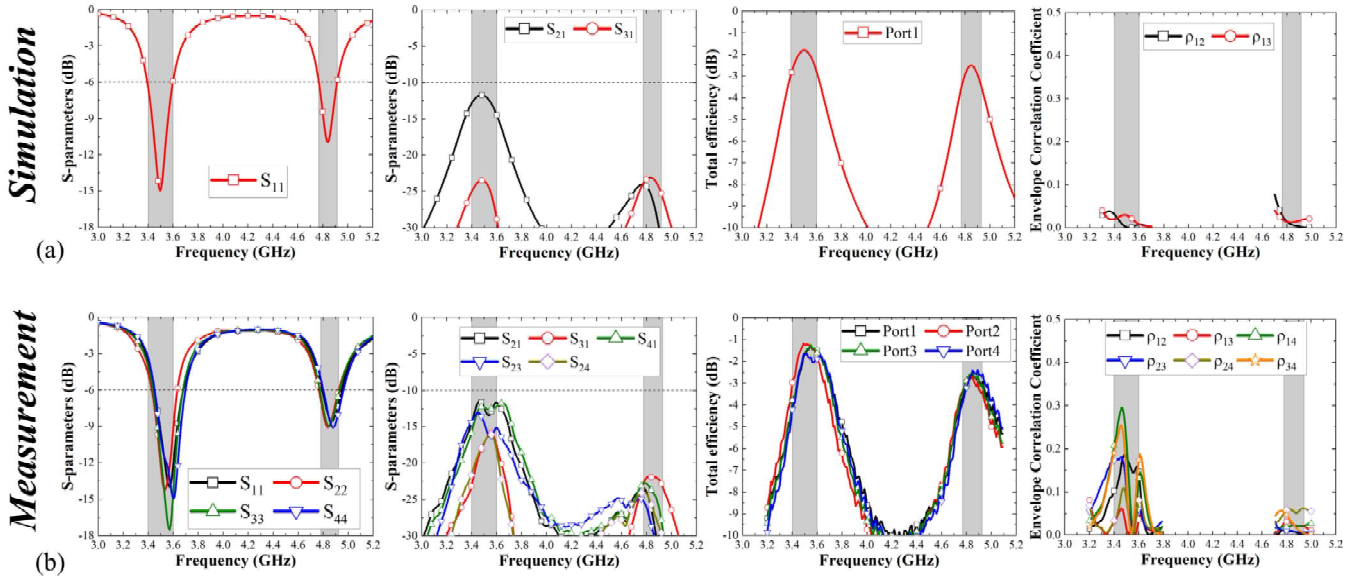

Fig. 3. (a) simulated and (b) measured results of the proposed dual-band 4×4 antenna module.

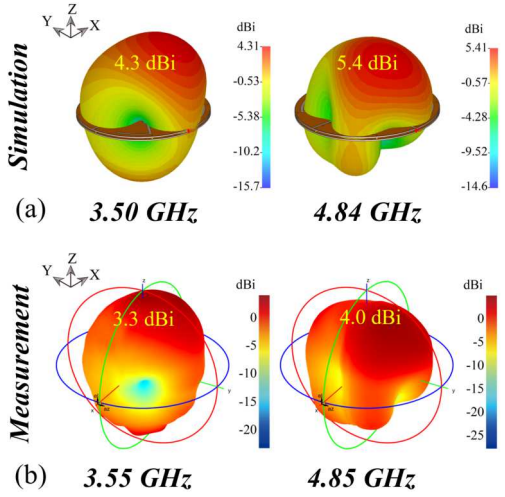

Fig. 4. (a) simulated and (b) measured 3D radiating pattern.

of Ant 1 is -2.2 dB (59.7%) and -3.0 dB (49.4%) for the lower band and higher band, respectively. The isolations are better than 11.8 dB and 24.0 dB for the adjacent elements (S_{21}), and 23.5 dB and 23.0 dB for the diagonal elements (S_{31}) across N78 and N79 band. ECCs at the target band is lower than 0.05.

In Fig. 3 (b), measured results of the fabricated prototype is shown, which basically agree with the simulation. The -6 dB impedance bandwidths are 3.43-3.68 GHz (250 MHz, 7.0%) and 4.76-4.93 GHz (170 MHz, 3.5%) with average efficiencies of -1.9 dB (64.3%) and -2.9 dB (51.3%) for the lower and higher bands, respectively. For the adjacent elements, the isolations (S_{21}, S_{41}, and S_{32}) are better than 11.5 dB and 22.8 dB across N78 and N79 band; for the diagonal elements, they (S_{31} and S_{42}) are better than 15.8 dB and 21.9 dB. ECCs are lower than 0.30 at the target band.

Fig. 4 shows the simulated and measured 3D radiating pattern of Ant 1, and they agree with each other well. The measured maximum realized gains are 3.3 dBi and 4.0 dBi at 3.55 GHz and 4.85 GHz, respectively. In a word, the measured results have verified the feasibility.

2.3 Operation Mechanism

Here, we analyze the field distribution of the Ant 1 to understand the dual-band operation mechanism. Each element can be divided into two parts, namely area A and area B. The frequency of 3.50 GHz is mainly radiated by region A, and the frequency of 4.84 GHz is mainly radiated by region B.

At 3.50 GHz, the field distribution is a one-eight quasi-TM_{11} mode of the circular patch. The electric field intensity gradually increases from zero to the maximum either along the circumference direction from the shorted pin beside the L-shaped slot to the straight open edge or along the radius direction from the circle center to the outer edge. The outer edge of area A is the main radiating aperture, and area A is the main radiating region.

At 4.85 GHz, the field distribution is a quasi-$TM_{0,0.5}$ mode of the half-mode patch. As can be seen from Fig. 5, the electric field intensity gradually increases from zero to the maximum from the straight shorted edge to the L-shaped slot, while it is almost uniform along the Y direction. The outer edge of area B is the main radiating aperture, and area B is the main radiating region. Due to rotation symmetry, the field distribution of Ant 2, 3 and 4 is identical to that of Ant 1, thus it will not be explained in detail here for the sake of conciseness.

3 Conclusion

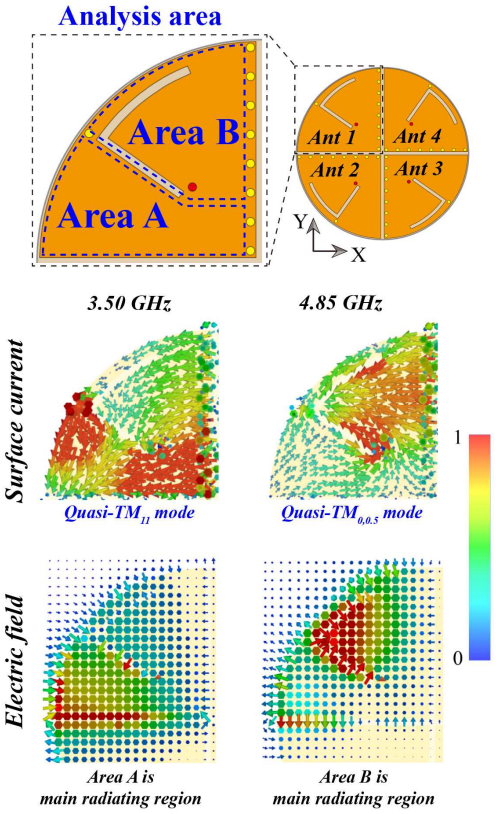

Fig. 5. 2D surface current and electric field distributions at (a) 3.5 GHz and (b) 4.85 GHz.

This paper focuses on the design of dual-band 4×4 antenna module with a low-profile property to cover Chinese 5G bands of N78/N79. By loading the shorting pins and etching an L-shaped slot, the proposed dual-mode PIFA operate with the one-eight quasi-TM_{11} mode of the circular patch and quasi-$TM_{0,0.5}$ mode of the half-mode patch. Presenting a circular shape, the proposed antenna module is with a dimension of $\pi \times 26^2$ mm^2. It exhibits great potential to be integrated with the back cover of modern 5G terminals.

4 Acknowledgement

This work was supported in part by the National Natural Science Foundation of China under Grant 62101427 and in part by the Key Research and Development Project of Shaanxi Province under Grant 2022GY-095, in part by the High-Level Innovation Talent Project Imported by QinChuangYuan of Shaanxi Province under Grant QCYRCXM-2022-33, and in part by the Shaanxi Key Laboratory of Deep Space Exploration Intelligent Information Technology under Grant No. 2021SYS-04.

References

[1] K. L. Wong and M. T. Chen, "Small-size LTE/WWAN printed loop antenna with an inductively coupled branch strip for bandwidth enhancement in the tablet computer," *IEEE Trans. Antennas Propag.*, vol. 61, no. 12, pp. 6144–6151, Sep. 2013.

[2] Y. L. Ban, Z. X. Chen, Z. Chen, K. Kang, and J. L. W. Li, "Decoupled closely spaced heptaband antenna array for WWAN/LTE smartphone applications," *IEEE Antennas Wireless Propag. Lett.*, vol. 13, pp. 31–34, Dec. 2014.

[3] D. Wu, S. W. Cheung, and T. I. Yuk, "A compact and low-profile loop antenna with multiband operation for ultra-thin smartphones," *IEEE Trans. Antennas Propag.*, vol. 63, no. 6, pp. 2745–2750, Jun. 2015.

[4] H. Xu, H. Y. Wang, S. Gao, H. Zhou, Y. Huang, Q. Xu, and Y. J. Cheng, "A compact and low-profile loop antenna with six resonant modes for LTE smartphone," *IEEE Trans. Antennas Propag.*, vol. 64, no. 9, pp. 3743–3751, Sep. 2016.

[5] I. R. R. Barani and K. L. Wong, "Integrated inverted-F and open-slot antennas in the metal-framed smartphone for 2 × 2 LTE LB and 4 × 4 LTE M/HB MIMO operations," *IEEE Trans. Antennas Propag.*, vol. 66, no. 10, pp. 5004–5012, Oct. 2018.

[6] I. R. R. Barani, K. L. Wong, Y. X. Zhang, and W. Y. Li, "Low-profile wideband conjoined open-slot antennas fed by grounded coplanar waveguides for 4×4 5G MIMO operation," *IEEE Trans. Antennas Propag.*, vol. 68, no. 4, pp. 2646–2657, Apr. 2020.

[7] L. Chang and H. Wang, "Miniaturized wideband four-antenna module based on dual-mode PIFA for 5G 4×4 MIMO applications," *IEEE Trans. Antennas Propag.*, vol. 69, no. 9, pp. 5297–5304, Sep. 2021.

[8] L. Peng, C. Ruan, and X. Wu, "Design and operation of dual/triple-band asymmetric M-shaped microstrip patch antennas," *IEEE Antennas Wireless Propag. Lett.*, vol. 9, pp. 1069–1072, Nov. 2010.

[9] K. Lee, S. Yang, and A. Kishk, "Dual- and multiband U-slot patch antennas," *IEEE Antennas Wireless Propag. Lett.*, vol. 7, pp. 645–647, Dec.2008.

[10] N. W. Liu, L. Zhu, Z. X. Liu, and Y. Liu, "Dual-band single-layer microstrip patch antenna with enhanced bandwidth and beamwidth based on reshaped multiresonant modes," *IEEE Trans. Antennas Propag.*, vol. 67, no. 11, pp. 7127–7132, Nov. 2019.

[11] J. Tak, S. Woo, J. Kwon, and J. Choi, "Dual-band dual-mode patch antenna for On-/Off-Body WBAN communications," *IEEE Antennas Wireless Propag. Lett.*, vol. 15, pp. 348–351, Jun. 2015.

[12] X. Chen, J. Wang and L. Chang, "Extremely Low Profile Dual Band Microstrip Patch Antenna Using Electric Coupling for 5G Mobile Terminal Application, *IEEE Trans. Antennas Propag.*, in press, 2022.

[13] J. Qian, F. Chen, and Q. Chu, "A novel tri-band patch antenna with broadside radiation and its application to filtering antenna," *IEEE Trans. Antennas Propag.*, vol. 66, no. 10, pp. 5080–5585, Oct. 2018.

[14] D. Yu, S. X. Gong, Y. T. Wan, and W. F. Chen, "Omnidirectional dual-band dual circularly polarized microstrip antenna using TM01 and TM02 modes," *IEEE Antennas Wireless Propag. Lett.*, vol. 13, pp. 1104–1107, Jun. 2014.